

Exploring the feasibility of the charged lepton flavor violating decay $\mu \rightarrow e + \gamma$ in inverse and linear seesaw mechanisms with A_4 flavour symmetry

Maibam Ricky Devi^{*} and Kalpana Bora[†]

Department of Physics, Gauhati University, Guwahati-781014, Assam, India

Abstract

One of the possible ways to explain the observed flavour structure of fundamental particles is to include flavor symmetries in the theories. In this work, we investigate the rare charged lepton flavour violating (cLFV) decay process ($\mu \rightarrow e\gamma$) in two of the low scale ($\sim \text{TeV}$) seesaw models: (i) the Inverse seesaw (ISS) and (ii) Linear seesaw (LSS) models within the framework of A_4 flavour symmetry. Apart from the A_4 flavour symmetry, some other symmetries like $U(1)_X$, Z_4 and Z_5 are included to construct the Lagrangian. We use results from our previous work [1, 2] where we computed unknown neutrino oscillation parameters within 3σ limits of their global best fit values, and apply those results to compute the branching ratio (BR) of the muon decay for both the seesaw models. Next we compare our results with the current experimental bounds and sensitivity limits of $\text{BR}(\mu \rightarrow e\gamma)$ as projected by various experiments, and present a comparative analysis that which of the two models is more likely to be tested by which current/future experiment. This is done for various values of currently allowed non-unitarity parameter. This comparative study will help us to pinpoint that which of the low scale seesaw models and triplet flavon VEV alignments will be more viable and favourable for testing under a common flavour symmetry (A_4 here), and hence can help discriminate between the two models.

^{*}Electronic address: deviricky@gmail.com

[†]Electronic address: kalpana@gauhati.ac.in

I. INTRODUCTION

The hunt for the charged lepton flavour violating (cLFV) decay $\mu \rightarrow e + \gamma$ is like finding a needle in a stack of hay and has been a challenging endeavour for particle physicists. Lepton family number is not conserved in transitions among families in these processes. In standard model (SM), lepton flavour is conserved at all orders of perturbation theory, but may get nonzero contributions through some beyond SM processes, like neutrino oscillation. The MEG (Mu to E Gamma) experiment [3, 4] (2008-2013) at the Paul Scherrer Institute (PSI), located at Villigen, Switzerland has set the most stringent upper limit on $BR(\mu \rightarrow e + \gamma) \leq 4.2 \times 10^{-13}$ at 90% C.L. in its first phase. This constraint would either validate or nullify models that predict the golden channel of cLFV decay, $\mu \rightarrow e + \gamma$ by incorporating physics beyond the Standard Model. The future sensitivity of this channel is expected to get enhanced up to an order of $BR(\mu \rightarrow e + \gamma) < 5.0 \times 10^{-14}$ by the upgraded version of MEG experiment, also popularly called MEG II experiment [5] which is currently in commissioning phase. The rare muon decay channel like $\mu \rightarrow e + \gamma$ is called “golden channel” - firstly due to the abundant rate of muon production in cosmic radiation as well as in accelerators and secondly because of its significantly longer lifetime than the rest of the leptons [6]. It is interesting to note that the cLFV processes can be related to neutrino oscillation, due to the mixing of neutrino flavour eigenstates within loop diagrams. It is known that though such cLFV decay rates are highly suppressed in SM, however get enhanced if there is mixing between light and heavy neutrino eigenstates. This linkage of neutrino mixing to cLFV processes can directly give us an unambiguous signature of new physics, and therefore has been of interest to the scientific community. Although the manifestation of new physics is quite unclear, its detection can open up a new portal to our understanding of baryon asymmetry of the universe, flavour structure of neutrino mixing etc.

Recently, an intense positive and negative muon beam facility powered by Proton Improvement Plan II, or PIP-II [7] is created in the Fermilab accelerator complex. The Advanced Muon Facility (AMF) [7] will drive cutting-edge research on studies related to cLFV to answer some of its most profound questions. The HiMB (High Intensity Muon Beam)[8] could further increase the sensitivity of MEG II experiment once it's ready for phase one. Hence theoretical studies related to $\mu \rightarrow e + \gamma$ become even more interesting

and relevant.

Keeping in view the above discussion on the importance of $\mu \rightarrow e + \gamma$ decays, in this work we compute and analyse the $BR(\mu \rightarrow e + \gamma)$ for different VEV alignments of A_4 triplet flavons, for linear (LSS) and inverse low-scale seesaw (ISS) models. Since high-scale seesaw models are not directly accessible to experiments, we choose low-scale seesaw models[1, 2]. Currently not much is known about symmetry breaking scale and VEV alignment etc. of A_4 flavour symmetry, also it is not clear which seesaw mechanism is more favourable. It is possible to obtain an observable cLFV decay rate satisfying the current experimental bounds and future sensitivity through neutrino oscillation, thus we can explore the feasibility of the two low-scale seesaw models for the detection of the cLFV decay under a common A_4 flavour symmetry. Some other similar works can be found in [9–16]. Through this work, one can also comment on which of the two models would be more favourable in context of BR of cLFV $\mu \rightarrow e + \gamma$ decay.

We proposed an inverse seesaw model in the Refs[1, 2], where we have studied the correlation between effective neutrino mass of $0\nu\beta\beta$ decay and $m_{lightest}$ by using the unknown neutrino oscillation data, i.e., $m_{lightest}$, δ_{CP} , α and β obtained from our model and their corresponding known neutrino oscillation parameters taken from recent global fit data [17]. Using these parameter data we have pinpointed the favored octant and mass hierarchy for the favored VEV alignment of the triplet scalar flavon involved in our model. In this work we have successfully pinpointed that for $(-1,1,1)/(1,-1,-1)$ VEV alignment of the triplet scalar flavon, the correlation between $m_{lightest}$ and effective neutrino mass of $0\nu\beta\beta$ aligns with the correlation plot of $m_{lightest}$ and $m_{0\nu\beta\beta}$ obtained from experimental global analysis. We also constructed the linear seesaw model in [1] where we have compared our previously mentioned ISS model and our linear model. One can find other A_4 flavour symmetry based neutrino models [18–21]. In [22, 23], an inverse as well as linear models are presented with detailed discussion of symmetries such as $SU(2)_L$, Z_3 and A_4 for model building. Many other seesaw based neutrino models are presented in [24, 25] where A_4 symmetry is exclusively used to construct neutrino model in a specific seesaw scenario.

To find the unknown neutrino oscillation parameters, i.e., $m_{lightest}$, δ_{CP} , α and β , we

have compared the light neutrino mass matrix obtained from each model with the light neutrino mass matrix, $m_\nu = U_{PMNS}^T m_{\nu diag} U_{PMNS}$ where U_{PMNS} is the PMNS mixing matrix. After comparison of these matrices, we get a set of equations for both NH and IH for 26 possible combinations of VEV alignment of the triplet scalar flavon (TSF) involved in the models. We then solve these equations simultaneously to find the unknown parameters. A parameter scan of the rest of the known neutrino parameters, i.e., mixing angles, squared mass differences, is done within the 3σ range of global fit data. We choose the solutions which are very precise by checking them with a tolerance of $< 10^{-5}$. This precision allow us to predict only a few favored VEV alignments in the TSF with specific mass hierarchy and octant of the atmospheric mixing angle θ_{23} .

To maintain the appropriate symmetries, the flavon VEVs must align in a specific manner which can be derived from the minimization of the full scalar potential. The so-called F-term alignment mechanism (as mentioned in Ref. [26]) is the most widely used technique for producing unique flavon VEVs. In a supersymmetric configuration, the flavons are intended to be coupled to so-called driving fields. Driving fields, like flavons, transform generally in a non-trivial fashion under the family symmetry G while remaining neutral under the SM gauge group. The F-term equations are frequently solved for the trivial vacuum, which is the vacuum configuration in which none of the flavons produce a VEV. By incorporating soft supersymmetry breaking effects, this can be avoided and it is possible to get more or less any VEV alignment.

In our work we have chosen the possible cases of VEV alignments through the minimization of the scalar potential. The minimization of the full scalar potential and its possible VEV alignments for both ISS and LSS models is shown in Appendices A.1 and A.2. For all the flavons in our setup, the most generic renormalizable potential that is invariant under $A_4 \times Z_4 \times Z_5 \times U(1)_X$ in case of ISS model and $A_4 \times Z_5 \times Z'_5$ for LSS model have been stated which on minimization with respect to the different components of the triplet scalar field Φ_s , gives us a set of equations. We can determine the possible VEV alignments of the triplet scalar flavon field by solving those set of equations. The allowed and unallowed cases of these VEV alignments of TSF is shown in Table (IV). The details of this are available in our earlier work [2].

This paper has been arranged as follows. In section II we present a brief introduction to charged lepton flavour violation $\mu \rightarrow e + \gamma$ decay. The ISS and LSS models that will be used are constructed and presented in details in section III. In section IV we discuss the numerical analysis to compute branching ratio of $\mu \rightarrow e + \gamma$ decay using the unknown neutrino oscillation parameters as computed in [2] in both the models. In section V we present the results and a discussion on them. Section VI contains summary and conclusions.

II. CLFV DECAY ($\mu \rightarrow e + \gamma$)

The charged lepton flavour violating transitions could provide us with a direct signature of new physics beyond the Standard Model. Search for such lepton flavour violating decay processes have been studied in a host of channels in ongoing experiments such as MEG collaboration at PSI. However, no cLFV decay processes have been detected so far, as their decay rates are highly suppressed. Out of various decay channels, the most sensitive transitions are the ones involving first and second generation of leptons especially muons, i.e., $\mu^+ \rightarrow e^+ + \gamma$, $\mu^- N \rightarrow e^- N$, $\mu^+ \rightarrow e^+ e^- e^+$ because of their abundance in cosmic radiation and particle accelerators [27]. The flavour structure of neutrino mass matrix can help understand the charged lepton flavour violation too. The decay rate of $\mu \rightarrow e + \gamma$ can be expressed as [28–36] :

$$BR(l_\alpha \rightarrow l_\beta \gamma) \approx \frac{\alpha_W^3 \sin^2 \theta_W m_{l_\alpha}^5}{256 \pi^2 M_W^4 \Gamma_{l_\alpha}} \left| \sum_{i=1}^9 \mathcal{K}_{\alpha i}^* \mathcal{K}_{\beta i} G \left(\frac{\mathcal{M}_i^2}{M_W^2} \right) \right|^2, \quad (1)$$

Here, the parameter $\alpha_W = g^2/4\pi$, and g represents weak coupling. Also, θ_W is the electroweak mixing angle, M_W is the mass of W^\pm boson, \mathcal{M}_i is the mass of neutrinos (both light and heavy neutrinos), m_{l_α} is the mass of the decaying charged lepton l_α and finally, Γ_{l_α} is the total decay width of the decaying charged lepton l_α . $\mathcal{K}_{(\alpha,\beta)i}$ ($\alpha = \mu, \beta = e$ with $i=1, \dots, 9$) define the elements of the matrix \mathcal{K} that block diagonalises the 9×9 neutrino mass matrix M_ν [35] of the inverse seesaw and linear seesaw models, and further analysis is shown later in sub-sections III A and III B respectively. The form factor $G(x)$ is [33–38] :

$$G(x) = -\frac{2x^3 + 5x^2 - x}{4(1-x)^3} - \frac{3x^3 \ln x}{2(1-x)^4}, \text{ where } x = \frac{\mathcal{M}_i^2}{M_W^2} \quad (2)$$

The matrix \mathcal{K} can be expressed as [35] :

$$\mathcal{K} = \begin{pmatrix} \mathbb{K} - \frac{1}{2}B^*B^T & B^* \\ -B^T & \mathbb{K} - \frac{1}{2}B^TB^* \end{pmatrix} \begin{pmatrix} U & 0 \\ 0 & V \end{pmatrix} \quad (3)$$

where U is the usual PMNS matrix that block diagonalises the light neutrinos and V is the unitary matrix that diagonalises the heavy right-handed neutrinos [35]. The full parametrisation of the 9×9 active sterile flavour mixing matrix can be found in [39].

As will be seen in the inverse seesaw model in Eqn. (26) in the following sections, we can repartition the 9×9 matrix into a type-I like matrix as

$$(M_\nu)_{iss} = \begin{pmatrix} 0 & M_D \\ M_D^T & M_R \end{pmatrix} \quad (4)$$

where

$$M_D = \begin{pmatrix} m_D & 0 \end{pmatrix}, M_R = \begin{pmatrix} 0 & M \\ M^T & \mu_s \end{pmatrix}, M_R^{-1} = \begin{pmatrix} -X^{-1} & M^{T-1} \\ M^{-1} & 0 \end{pmatrix} \quad (5)$$

$$\text{where, } X = M\mu_s^{-1}M^T.$$

Similarly in the case of linear seesaw model, we can repartition Eqn. (19) as

$$(M_\nu)_{lss} = \begin{pmatrix} 0 & M'_D \\ M'^T_D & M'_R \end{pmatrix} \quad (6)$$

where,

$$\begin{aligned} M'_D &= \begin{pmatrix} M_D & M_L \end{pmatrix} \text{ and } M'_R = \begin{pmatrix} 0 & M \\ M^T & 0 \end{pmatrix} \\ \Rightarrow M'^{-1}_R &= \begin{pmatrix} 0 & M^{T-1} \\ M^{-1} & 0 \end{pmatrix} \end{aligned} \quad (7)$$

In Eqn. (3), the entry B acts a small perturbation matrix which can expressed as [35]:

$$B = M_D M_R^{-1} = (m_D M^{T-1} \mu_s M^{-1}, m_D M^{T-1}) \quad (\text{in case of ISS}) \quad (8)$$

$$B = M'_D M'^{-1}_R = (M_L M^{-1}, M_D M^{T-1}) \quad (\text{in case of LSS}) \quad (9)$$

The matrix V can be numerically computed as [35, 40]

$$V = \frac{\sqrt{2}}{2} \begin{pmatrix} \mathbb{K}_3 & -i\mathbb{K}_3 \\ \mathbb{K}_3 & i\mathbb{K}_3 \end{pmatrix} + \mathcal{O}(\mu_s M^{-1}) \quad (10)$$

Experiments	Year	Upper Limit	Ref.
MEG	2016	4.2×10^{-13}	[3, 4]
MEG II	Commissioned in 2017	5.0×10^{-14} *	[5]
AMF (PIP II in FermiLab)	2022	(In planning stage) **	[7]

TABLE I: *Current upper limit (MEG) and future sensitivity of $BR(\mu \rightarrow e + \gamma)$ set by various experiments. (*) indicates the future sensitivity of MEG II experiment, and (**) that of the the Advanced Muon Facility.*

The matrix element μ_s is absent in the neutrino mass matrix of linear seesaw model. The matrix $\mathcal{K}_{3 \times 3}$ is related to the parameter η [35] that represents deviation from unitarity (for both ISS and LSS models) as

$$\mathcal{K}_{3 \times 3} = (\mathbb{K} - \frac{1}{2} B_i^* B_i^T) U = (\mathbb{K} - \eta) U \quad (11)$$

$$\text{where, } \eta = \frac{1}{2} B_i^* B_i^T = \frac{1}{2} |M_D M^{T-1}|^2 \quad (12)$$

III. THE MODELS

As stated earlier, this work aims to constrain and compare the ISS and LSS models with A_4 flavour symmetry with reference to the cLFV decay ($\mu \rightarrow e + \gamma$), and to check their testability and viability at ongoing/future planned experiments. To compute the branching ratio of the muon decay, we use these models with A_4 symmetry from our previous works [1, 2].

A. Inverse seesaw model

The 9×9 neutrino mass matrix in the basis (ν_L^c, N, S) obtained from inverse seesaw (ISS) mechanism is [41]

$$M_\nu = \begin{bmatrix} 0 & M_D & 0 \\ M_D^T & 0 & M \\ 0 & M^T & \mu_s \end{bmatrix}. \quad (13)$$

We present here the ISS model, for the sake of completeness of the work, that contains a $SU(2)_L$ singlet right-handed neutrino N along with three other singlet fermions $S_{i=1,2,3}$ (Sterile neutrinos) apart from the Standard Model particles. The particle content of this model under $A_4 \times Z_4 \times Z_5 \times U(1)_X$ symmetry is given in the Table II below [1, 2].

In Table (II) L and \mathcal{H} represents the charged lepton family and the $SU(2)_L$ Higgs doublet

	L	\mathcal{H}	e_R	μ_R	τ_R	N	S	Φ_T	Φ_s	Ω	ξ	τ	ρ	ρ'	ρ''
A_4	3	1	1	$1''$	$1'$	3	3	3	3	1	$1'$	$1''$	1	1	1
Z_4	1	1	i	i	i	i	1	i	-i	-i	-i	-i	i	i	1
Z_5	1	1	ω	ω	ω	ω^2	1	ω	1	1	1	1	ω^2	1	1
$U(1)_X$	-1	0	-1	-1	-1	-1	1	0	-1	-1	-1	-1	0	-4	-3

TABLE II: *Particle content for inverse seesaw model under $A_4 \times Z_4 \times Z_5 \times U(1)_X$ symmetry [1, 2]*

respectively, whereas, Ω , ξ , τ , ρ , ρ' and ρ'' are the A_4 singlet flavons and Φ_s is the A_4 triplet scalar. We choose the vev of flavon ϕ_T as $\langle \phi_T \rangle = v_T(1, 0, 0)$ [26] so that the charged lepton mass matrix turns out to be diagonal in the leading order as $M_l = v_h \frac{v_T^\dagger}{\Lambda} \text{diag}(Y_e, Y_\mu, Y_\tau)$ where Y_e , Y_μ , Y_τ represent the Yukawa coupling constants. The relevant Lagrangian for the neutrino sector is given as:

$$\mathcal{L}_Y \supset Y_D \frac{\bar{L} \tilde{H} N \rho^\dagger}{\Lambda} + Y_M N S \rho^\dagger + Y_{\mu_s} S S \left[\frac{\rho' \rho''^\dagger (\Phi_s + \Omega + \xi + \tau)}{\Lambda^2} \right] + h.c., \quad (14)$$

Using above equation, the mass matrix elements in Eqn. (13) can be written in the form as:

$$M_D = \frac{Y_D v_h v_\rho^\dagger}{\Lambda} \begin{bmatrix} 1 & 0 & 0 \\ 0 & 0 & 1 \\ 0 & 1 & 0 \end{bmatrix}, \quad M = Y_M v_\rho^\dagger \begin{bmatrix} 1 & 0 & 0 \\ 0 & 0 & 1 \\ 0 & 1 & 0 \end{bmatrix}, \quad (15)$$

$$\text{and, } \mu_s = \frac{Y_{\mu_s} v_{\rho'} v_{\rho''}^\dagger}{\Lambda^2} \begin{pmatrix} v_\Omega + 2v_s \phi_a & v_\xi - v_s \phi_c & v_\tau - v_s \phi_b \\ v_\xi - v_s \phi_c & v_\tau + 2v_s \phi_b & v_\Omega - v_s \phi_a \\ v_\tau - v_s \phi_b & v_\Omega - v_s \phi_a & v_\xi + 2v_s \phi_c \end{pmatrix}. \quad (16)$$

Here, Λ is the usual cutoff scale of the theory. Y_D, Y_M, Y_{μ_s} are the dimensionless coupling constants which are usually complex. The non-zero VEVs of scalars can be represented as: $\langle \mathcal{H} \rangle = v_h, \langle \Omega \rangle = v_\Omega, \langle \rho \rangle = v_\rho, \langle \rho' \rangle = v_{\rho'}, \langle \rho'' \rangle = v_{\rho''}, \langle \xi \rangle = v_\xi, \langle \tau \rangle = v_\tau, \langle \Phi_S \rangle = v_s(\Phi_a, \Phi_b, \Phi_c)$. The light neutrino mass matrix for inverse seesaw model is computed as [41] :

$$m_\nu = M_D(M^T)^{-1}\mu_s M^{-1}M_D^T. \quad (17)$$

Next, using the matrix elements of Eq.(14) into Eq.(17), the light neutrino mass matrix is obtained as,

$$\Rightarrow m_\nu = F_1 \begin{pmatrix} v_\Omega + 2v_s\phi_a & v_\xi - v_s\phi_c & v_\tau - v_s\phi_b \\ v_\xi - v_s\phi_c & v_\tau + 2v_s\phi_b & v_\Omega - v_s\phi_a \\ v_\tau - v_s\phi_b & v_\Omega - v_s\phi_a & v_\xi + 2v_s\phi_c \end{pmatrix}, \quad (18)$$

where, $F_1 = \frac{Y_D^2 Y_{\mu_s}}{Y_M^2} [\frac{v_h^2 v_{\rho'} v_{\rho''}^\dagger}{\Lambda^4}]$.

B. Linear seesaw model

The neutrino mass matrix using linear seesaw (LSS) mechanism [42, 43] with the basis (ν_L, N_R^c, S_R^c) is given as

$$M_\nu = \begin{bmatrix} 0 & M_D & M_L \\ M_D^T & 0 & M \\ M_L^T & M^T & 0 \end{bmatrix}. \quad (19)$$

For the LSS model we use $A_4 \times Z_5 \times Z'_5$ symmetries to generate the tiny but non-zero neutrino masses. The A_4 singlet flavons are $(\varepsilon, \kappa, \zeta, \varphi, \varphi')$, and other fields of the model under $A_4 \times Z_5 \times Z'_5$ symmetry such as A_4 triplet scalar Φ_s , $SU(2)_L$ charged lepton doublets L and $SU(2)_L$ Higgs doublet \mathcal{H} are shown in Table III. The effective light neutrino mass matrix formula for linear seesaw is given as [44],

$$m_\nu = M_D(M_L M^{-1})^T + (M_L M^{-1})M_D^T. \quad (20)$$

Taking into consideration the transformation of the neutrino fields under $A_4 \times Z_5 \times Z'_5$ symmetry and its interaction with the other fields, the Lagrangian of the neutrino sector

	L	\mathcal{H}	e_R	μ_R	τ_R	\mathcal{N}	\mathcal{S}	ε	Φ_T	Φ_s	κ	ζ	φ	φ'
A_4	3	1	1	1''	1'	3	3	1	3	3	1	1'	1''	1
Z_5	ω	1	ω	ω	ω	ω^2	ω^3	ω	1	ω^2	ω^2	ω^2	ω^2	1
Z'_5	ω	1	ω	ω	ω	ω	ω^2	1	1	ω	ω	ω	ω	ω^2

TABLE III: *Particle content for linear seesaw model under $A_4 \times Z_5 \times Z'_5$ symmetry*

can be now be written as:

$$\mathcal{L}_\nu \supset Y_D \frac{\bar{L} \tilde{\mathcal{H}} N \varepsilon^\dagger}{\Lambda} + Y_M N S \varphi' + Y_L \frac{\bar{L} \tilde{\mathcal{H}} S}{\Lambda} (\Phi_s^\dagger + \kappa^\dagger + \zeta^\dagger + \varphi^\dagger). \quad (21)$$

The mass matrix elements in Eqn. (19) become:

$$M_D = \frac{Y_D v_h v_\varepsilon^\dagger}{\Lambda} \begin{bmatrix} 1 & 0 & 0 \\ 0 & 0 & 1 \\ 0 & 1 & 0 \end{bmatrix}, \quad M = Y_M v_{\varphi'} \begin{bmatrix} 1 & 0 & 0 \\ 0 & 0 & 1 \\ 0 & 1 & 0 \end{bmatrix}, \quad (22)$$

$$M_L = \frac{Y_L v_h}{\Lambda} \begin{bmatrix} 2v_s^\dagger \Phi_a + v_\kappa^\dagger & -v_s^\dagger \Phi_c + v_\varphi^\dagger & -v_s^\dagger \Phi_b + v_\zeta^\dagger \\ -v_s^\dagger \Phi_c + v_\varphi^\dagger & 2v_s^\dagger \Phi_b + v_\zeta^\dagger & -v_s^\dagger \Phi_a + v_\kappa^\dagger \\ -v_s^\dagger \Phi_b + v_\zeta^\dagger & -v_s^\dagger \Phi_a + v_\kappa^\dagger & 2v_s^\dagger \Phi_c + v_\varphi^\dagger \end{bmatrix}. \quad (23)$$

The matrix elements from Eqn. (21) when used in Eq. (20) yield the light neutrino mass matrix as:

$$m_\nu = F_2 \begin{bmatrix} 2v_s^\dagger \Phi_a + v_\kappa^\dagger & -v_s^\dagger \Phi_c + v_\varphi^\dagger & -v_s^\dagger \Phi_b + v_\zeta^\dagger \\ -v_s^\dagger \Phi_c + v_\varphi^\dagger & 2v_s^\dagger \Phi_b + v_\zeta^\dagger & -v_s^\dagger \Phi_a + v_\kappa^\dagger \\ -v_s^\dagger \Phi_b + v_\zeta^\dagger & -v_s^\dagger \Phi_a + v_\kappa^\dagger & 2v_s^\dagger \Phi_c + v_\varphi^\dagger \end{bmatrix}, \quad (24)$$

where, $F_2 = \frac{2Y_L Y_D v_h^2 v_\varepsilon^\dagger}{\Lambda^2 Y_M v_{\varphi'}}$ is a dimensionless constant.

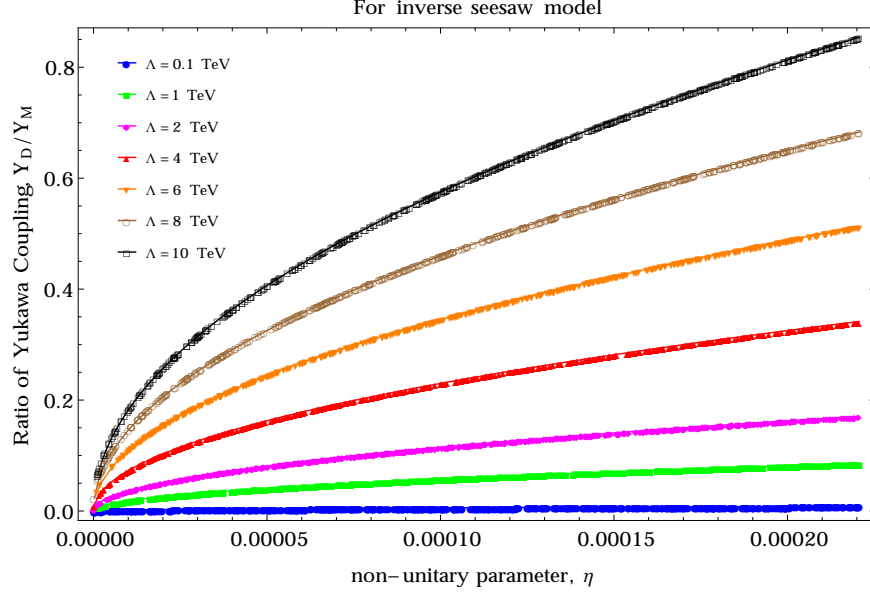


FIG. 1: Correlation plots between a and non-unitary parameter η for different values of Λ

IV. NUMERICAL ANALYSIS

The global-fit analysis constrains the non-unitary parameter [45, 46] as

$$|\eta| < \begin{pmatrix} 1.25 \times 10^{-3} & 1.20 \times 10^{-5} & 1.35 \times 10^{-3} \\ 1.20 \times 10^{-5} & 2.21 \times 10^{-4} & 6.13 \times 10^{-4} \\ 1.35 \times 10^{-3} & 6.13 \times 10^{-4} & 2.81 \times 10^{-3} \end{pmatrix}. \quad (25)$$

Since both of our A_4 symmetry based inverse and linear seesaw models predict $M_D M^{-1}$ to be a diagonal matrix, from Eqn. (25) we choose the strongest experimental bound of η as the constraint for our models, i.e., $\eta < 2.21 \times 10^{-4}$. We randomly choose four different values of η which satisfy the constraint $< \mathcal{O}(10^{-4})$ and use it to find the branching ratio of $BR(\mu \rightarrow e + \gamma)$ for the three allowed VEV alignments of the triplet flavon Φ_s (0,1,1) (NH), (-1,1,1) (NH) and (0,1,-1) (IH). It may be noted that in our previous work [2], only for these three cases we had obtained the neutrino oscillation parameters within the 3σ ranges of their current allowed global best fit values. We do the analysis for four randomly chosen (and allowed) values of the non-unitarity parameter $\eta = 2.19 \times 10^{-4}$, $\eta = 4.0 \times 10^{-6}$, $\eta = 5.0 \times 10^{-7}$ and $\eta = 9.0 \times 10^{-9}$.

SL. NO.	VEV	ISS/LSS		SL. NO.	VEV	ISS/LSS	
		NH	IH			NH	IH
1	(1,0,0)	X	X	14	(-1,1,-1)	X	X
2	(0,1,0)	X	X	15	(-1,-1,1)	X	X
3	(0,0,1)	X	X	16	(1,1,-1)	X	X
4	(1,1,0)	X	X	17	(1,-1,1)	X	X
5	(1,0,1)	X	X	18	(-1,1,1)	allowed	X
6	(0,1,1)	allowed	X	19	(-1,-1,0)	X	X
7	(1,-1,0)	X	X	20	(-1,0,-1)	X	X
8	(1,0,-1)	X	X	21	(0,-1,-1)	allowed	X
9	(-1,0,1)	X	X	22	(-1,0,0)	X	X
10	(-1,1,0)	X	X	23	(0,-1,0)	X	X
11	(0,-1,1)	X	allowed	24	(0,0,-1)	X	X
12	(0,1,-1)	X	allowed	25	(1,1,1)	X	X
13	(1,-1,-1)	allowed	X	26	(-1,-1,-1)	X	X

TABLE IV: Summary of our result after solving the triplet flavon equations of different VEV alignments for all the inverse and linear seesaw mechanisms. The green sign, X indicate ruled out cases, where no output is obtained for the tolerance level of 10^{-5} .

A. Numerical analysis for Inverse seesaw model

We know that for Inverse seesaw model [40, 41],

$$m_\nu = M_D(M^T)^{-1}\mu_s M^{-1}M_D^T \Rightarrow m_\nu = F\mu_s F^T \quad (26)$$

$$\text{where, } F = M_D M^{-1} \Rightarrow F = \mathbb{C}|I_{3 \times 3}| ; \mathbb{C} = \frac{Y_D v_h}{\Lambda Y_M} \quad (27)$$

From Eqn.(26) we have

$$m_\nu = |\mathbb{C}|^2 \mu_s \Rightarrow \mu_s = \frac{m_\nu}{|\mathbb{C}|^2} = \frac{U_{pmns} m_{\nu_{diag}} U_{pmns}^T}{|\mathbb{C}|^2} \quad (28)$$

$$\text{Since, } \eta = \frac{1}{2} F F^\dagger \Rightarrow \eta = \frac{1}{2} |\mathbb{C}|^2 I_{3 \times 3} \quad (29)$$

From Eqns.(28) and (29), we can write

$$\mu_s = \frac{U_{pmns} m_{\nu_{diag}} U_{pmns}^T}{2\eta}. \quad (30)$$

Also, for the three allowed cases of VEV alignment of triplet flavon field Φ_s , the matrix μ_s from Eqn. (16) takes the following different forms:

1. For VEV (0,1,1) with normal hierarchy:

$$\mu_s = K_1 \begin{bmatrix} A_1 & B_1 - 1 & C_1 - 1 \\ B_1 - 1 & C_1 + 2 & A_1 \\ C_1 - 1 & A_1 & B_1 + 2 \end{bmatrix}, \quad (31)$$

where, $K_1 = \left| \frac{Y_{\mu_s} v_{\rho'} v_{\rho''}^\dagger v_s}{\Lambda^2} \right|$, $A_1 = \left| \frac{v_\Omega}{v_s} \right|$, $B_1 = \left| \frac{v_\xi}{v_s} \right|$ and $C_1 = \left| \frac{v_\tau}{v_s} \right|$.

2. For VEV (-1,1,1) with normal hierarchy:

$$\mu_s = K_1 \begin{bmatrix} A_1 - 2 & B_1 - 1 & C_1 - 1 \\ B_1 - 1 & C_1 + 2 & A_1 + 1 \\ C_1 - 1 & A_1 + 1 & B_1 + 2 \end{bmatrix}, \quad (32)$$

3. For VEV (0,1,-1) with inverted hierarchy:

$$\mu_s = K_1 \begin{bmatrix} A_1 & B_1 + 1 & C_1 - 1 \\ B_1 + 1 & C_1 + 2 & A_1 \\ C_1 - 1 & A_1 & B_1 - 2 \end{bmatrix}, \quad (33)$$

where, A_1 , B_1 and C_1 take same form in all the three cases above. We use the randomly chosen value of η in Eqn. (30), and then comparing it with Eqns. (31), (32) and (33), the elements A_1 , B_1 and C_1 can be computed, with the assumption for simplicity that $|K_1| \sim 1$ eV in further analysis. We take all the non-zero elements of the matrix M in Eqn. (15) of the order of ~ 1 TeV. The heavy Majorana neutrinos M_R which is an admixture of basis N and S have mass eigenvalues given by $M_R = M \pm \frac{\mu_s}{2}$ [35, 47] whose values are used in Eqn.(1).

Further, the Dirac Matrix M_D can be constructed, for inverse seesaw mechanism[33] as,

$$M_D = U m_{\nu diag}^{1/2} \mathcal{R} \mu_s^{-1/2} M^T \quad (34)$$

\mathcal{R} being a complex orthogonal matrix satisfying $\mathcal{R}\mathcal{R}^T = \mathbb{1}_{3 \times 3}$. We next calculate B as given in Eqns. (3) and (8) and use the values of \mathcal{K} from Eqn. (3) to compute the branching ratio in Eqn.(1). Since $M_D M^{-1} = \left(\frac{Y_D v}{\Lambda Y_M} \right) \mathbb{1}_{3 \times 3}$, from Eqns. (8) and (12), we can write

$$|\eta| = \frac{1}{2} \left[\frac{Y_D v_h}{\Lambda Y_M} \right]^2 \mathbb{1}_{3 \times 3} \approx \frac{a^2}{2} \left[\frac{v_h}{\Lambda} \right]^2 \mathbb{1}_{3 \times 3} \quad (35)$$

where $a = \frac{Y_D}{Y_M}$, and Y_D and Y_M are Yukawa couplings of the L-N and N-S sectors respectively. At present, no information is available on Y_D , Y_M or Λ and the cut-off scale of (and hence flavour symmetry breaking scale) the theory Λ can take different possible values. However, constraints on the value of non-unitarity parameter η is available, and hence relation in Eqn. (31) can be used to obtain a correlation plot between the parameter “a” and the non-unitary parameter η , which is shown in Fig (1) for different values of the cutoff scale Λ . This graph depicts that same value non-unitarity parameter η can be obtained for different values of ratio of couplings $\frac{Y_D}{Y_M}$ if cut-off scale of the theory can be fine tuned. This also implies that same amount of non-unitarity can be generated for different values of scale of flavour symmetry breaking, if $\frac{Y_D}{Y_M}$ can be adjusted accordingly. In other words, it can be stated that all the physical quantities Λ, Y_M , and Y_D can not be allowed to change freely in order to generate a given amount of non-unitarity. Also, the curve with the steeper slope indicates variation of Y_D/Y_M with respect to non-unitary parameter η for a given cut-off scale Λ having higher value than that for the lower curve. The higher the value of Λ , higher is the value of the ratio Y_D/Y_M for a given non-unitary parameter within its allowed region of ($0 < \eta < 2.2099 \times 10^{-4}$).

B. Numerical analysis for Linear seesaw model

From Eqn.(20), it is seen that the mass matrix M_L can be obtained as:

$$|M_L| = \left| \frac{m_\nu}{2M_D M^{-1}} \right| \quad (36)$$

$$\Rightarrow |M_L| = \left| \frac{U_{pmns} m_{\nu diag} U_{pmns}^T}{2\sqrt{2}\eta} \right| \text{ where, } \eta = \frac{1}{2} \left| M_D M^{-1} \right|^2 \quad (37)$$

For this model, the M_L mass matrix from Eqn. (23) for the three allowed vacuum alignments of the triplet flavon Φ_s can be reduced to the following form:

1. For VEV (0,1,1) with normal hierarchy:

$$M_L = K_2 \begin{bmatrix} A_2 & B_2 - 1 & C_2 - 1 \\ B_2 - 1 & C_2 + 2 & A_2 \\ C_2 - 1 & A_2 & B_2 + 2 \end{bmatrix}, \quad (38)$$

where, $K_2 = \left| \frac{Y_L v_h v_s^\dagger}{\Lambda} \right|$, $A_2 = \left| \frac{v_\kappa^\dagger}{v_s^\dagger} \right|$, $B_2 = \left| \frac{v_\zeta^\dagger}{v_s^\dagger} \right|$ and $C_2 = \left| \frac{v_\varphi^\dagger}{v_s^\dagger} \right|$.

2. For VEV (-1,1,1) with normal hierarchy:

$$M_L = K_2 \begin{bmatrix} A_2 - 2 & B_2 - 1 & C_2 - 1 \\ B_2 - 1 & C_2 + 2 & A_2 + 1 \\ C_2 - 1 & A_2 + 1 & B_2 + 2 \end{bmatrix}, \quad (39)$$

3. For VEV (0,1,-1) with inverted hierarchy:

$$M_L = K_2 \begin{bmatrix} A_2 & B_2 - 1 & C_2 + 1 \\ B_2 - 1 & C_2 - 2 & A_2 \\ C_2 + 1 & A_2 & B_2 + 2 \end{bmatrix}, \quad (40)$$

In Eqn (33), we feed the chosen value for η , and then Eqns. (38), (39), (40) are compared with Eqn. (36) to find the elements A_2 , B_2 and C_2 by taking $|K_2| \sim 1$ eV for simplicity. We assume all the non-zero elements of M to be ~ 1 TeV where the heavy Majorana neutrino mass matrix $M_R = \pm M$ [35]. The Dirac mass matrix M_D is computed as [33],

$$M_D = |U m_{\nu diag}^{1/2} \mathcal{R}' m_{\nu diag}^{1/2} U^T M_L^{-1} M^T| \quad (41)$$

where, \mathcal{R}' satisfies $\mathcal{R}' + \mathcal{R}'^T = \mathbb{K}_{3 \times 3}$. For further details, one can refer to [32, 33, 35]. This

is then used in Eqn. (11) and Eqn. (1) to compute the branching ratio of $\mu \rightarrow e + \gamma$ for the four values of non-unitary parameter η . We would like to note that correlation plots similar to Fig. 1 can also be obtained for LSS model. Our results based on this analysis are presented and discussed in Section 5.

C. Dynamics of flavour symmetry

For ISS model as given in section (III A), we can consider the typical energy scales of the different mass matrices as - $M_D = 10$ GeV, $M = 1$ TeV, $v_h = 246$ GeV. This gives $\frac{v_h}{\Lambda} = 2.46 \times 10^{-4} \approx 2.5 \times 10^{-4}$ for a cut-off scale of $\Lambda = 10^3$ TeV. From Eqns.(15) and (16), we can write:

$$\frac{M_D}{M} = \left(\frac{Y_D}{Y_M} \right) \left(\frac{v_h}{\Lambda} \right) \approx 10^{-2} \quad (42)$$

and we get

$$Y_M = 0.025 Y_D \quad (43)$$

Using the chosen values $K_1 = 1$ eV $Y_{\mu_s} \sim 0.01$, one gets

$$v_{\rho'} v_{\rho''}^\dagger v_s = 10^{-4} (\text{TeV})^3 \quad (44)$$

This condition can be satisfied by taking a set of values for the flavon VEVs and coupling constants as shown in Table (??) without affecting the overall gauge symmetries and interactions considered in the model. For this set of values we get $A_1 \sim 2000$, $B_1 \sim 1500$ and $C_1 \sim 1000$ which agree with some typical values of A_1 , B_1 and C_1 from their actual data obtained in our computation. Proceeding similarly for the LSS model, considering the energy scales $M_D = 10$ GeV, $M = 1$ TeV, $M_L = 10$ eV and $\Lambda = 10^3$ TeV, we can evaluate from Eqns. (22) and (23) as

$$\frac{M_D}{M} = 10^{-2} \Rightarrow \frac{Y_D v_\epsilon^\dagger}{Y_M v_{\varphi'}} \times 2.5 \times 10^{-2} = 1 \quad (45)$$

and it can be shown that

$$\frac{v_\epsilon^\dagger}{v_{\varphi'}} > 1 \quad (46)$$

Non-unitary parameter, η	VEV	NH/IH	Type	Range of $BR(\mu \rightarrow e + \gamma)$	Experiments that can probe
2.19×10^{-4}	(0,1,1)	NH	ISS	$1.2362 \times 10^{-7} \rightarrow 2.87721 \times 10^{-7}$	T, S, E, CB, M^* , M, MII, NG
		NH	LSS	$1.00088 \times 10^{-10} \rightarrow 6.51129 \times 10^{-10}$	E, CB, M^* , M, MII, NG
	(-1,1,1)	NH	ISS	$9.82583 \times 10^{-9} \rightarrow 5.50333 \times 10^{-7}$	T, S, E, CB, M^* , M, MII, NG
		NH	LSS	$9.05723 \times 10^{-13} \rightarrow 1.39745 \times 10^{-12}$	M, MII, NG
	(0,1,-1)	IH	ISS	$2.8648 \times 10^{-9} \rightarrow 9.51365 \times 10^{-8}$	T, S, E, CB, M^* , M, MII, NG
		IH	LSS	$6.54537 \times 10^{-8} \rightarrow 1.19193 \times 10^{-7}$	T, S, E, CB, M^* , M, MII, NG
4.0×10^{-6}	(0,1,1)	NH	ISS	$4.39094 \times 10^{-11} \rightarrow 9.32741 \times 10^{-11}$	CB, M^* , M, MII, NG
		NH	LSS	$1.2099 \times 10^{-12} \rightarrow 5.33457 \times 10^{-12}$	M, MII, NG
	(-1,1,1)	NH	ISS	$2.54968 \times 10^{-12} \rightarrow 1.47428 \times 10^{-10}$	CB, M^* , M, MII, NG
		NH	LSS	$1.12946 \times 10^{-12} \rightarrow 2.1398 \times 10^{-12}$	M^* , M, MII, NG
	(0,1,-1)	IH	ISS	$7.78198 \times 10^{-13} \rightarrow 3.21865 \times 10^{-11}$	M^* , M, MII, NG
		IH	LSS	$3.41281 \times 10^{-11} \rightarrow 4.84894 \times 10^{-11}$	M^* , M, MII, NG
5.0×10^{-7}	(0,1,1)	NH	ISS	$6.87031 \times 10^{-13} \rightarrow 1.45709 \times 10^{-12}$	M, MII, NG
		NH	LSS	$9.8222 \times 10^{-13} \rightarrow 3.17343 \times 10^{-11}$	M^* , M, MII, NG
	(-1,1,1)	NH	ISS	$4.04261 \times 10^{-14} \rightarrow 2.29969 \times 10^{-12}$	M, MII, NG
		NH	LSS	$7.6931 \times 10^{-12} \rightarrow 7.90733 \times 10^{-11}$	CB, M^* , M, MII, NG
	(0,1,-1)	IH	ISS	$1.2138 \times 10^{-14} \rightarrow 5.03077 \times 10^{-13}$	M, MII, NG
		IH	LSS	$9.23256 \times 10^{-13} \rightarrow 1.42411 \times 10^{-12}$	M, MII, NG
9.0×10^{-9}	(0,1,1)	NH	ISS	$2.22641 \times 10^{-16} \rightarrow 4.72084 \times 10^{-16}$	NG
		NH	LSS	$7.77436 \times 10^{-15} \rightarrow 1.94312 \times 10^{-17}$	NG
	(-1,1,1)	NH	ISS	$1.3125 \times 10^{-17} \rightarrow 7.44927 \times 10^{-17}$	NG
		NH	LSS	$3.357874 \times 10^{-15} \rightarrow 8.46285 \times 10^{-15}$	NG
	(0,1,-1)	IH	ISS	$3.93177 \times 10^{-18} \rightarrow 1.63004 \times 10^{-16}$	NG
		IH	LSS	$3.32112 \times 10^{-16} \rightarrow 5.74934 \times 10^{-16}$	NG

TABLE V: Results of this work on Branching Ratio of the $cLFV$ decay $\mu \rightarrow e + \gamma$ for allowed vacuum alignments of the triplet flavon, for ISS and LSS models and the different experiments that can probe them. Here NH and IH represents normal and inverted hierarchies respectively. The color codes indicates ■ \rightarrow NH (Normal Hierarchy), ■ \rightarrow IH (Inverted Hierarchy), ■ \rightarrow ISS (Inverse Seesaw), ■ \rightarrow LSS (Linear Seesaw). ■ represents the dataset for which the upper limit of $BR(\mu \rightarrow e + \gamma)$ falls in the current limit of MEG and future sensitivity of MEG II. Here the experiments are indexed as T for TRIMUF, S for SIN, E for E328, CB for Crystal Box, M^* for MEGA, M for MEG, MII for MEG II and NG for next generation muon beam experiments such as AMF in Fermilab. The experiments such as TRIUMF, SIN, E328, Crystal Box and MEGA are not operating currently and MEG and MEG II are the currently active experiments. Here NG means next-generation experiments.

Also, using the chosen value $K_2 = 1$ eV in section (III B), we get

$$K_2 = \frac{Y_L v_h v_s^\dagger}{\Lambda} \Rightarrow Y_L v_h v_s^\dagger = 4 \text{ keV} , \text{ (where } \Lambda = 10^3 \text{ TeV)} \quad (47)$$

Eqns (46) and (47) can be satisfied by choosing a set of values as shown in Table (??). Using these values, we obtain $A_2 = B_2 = C_2 = 10$ which agrees with of the values of A_2 , B_2 and C_2 obtained from computation.

For above set of scales and couplings, m_ν is obtained in the sub-eV range. For LSS, the constants A_2 , B_2 and C_2 are computed to be of the order of 10, two orders of magnitude smaller than those of ISS model. It may be noted that we showed this analysis for scales and couplings for some chosen values for demonstration purpose, and can be done for their other values also, such that they satisfy various constraints. Hence, it is seen that flavons corresponding to different representations of A_4 group obtain VEVs across a range of scales, and the flavour symmetry breaking exhibits a very rich and dynamic structure in the two models. Also, it is seen that

$$\frac{\mu_S(= 1keV)}{M_L(= 10eV)} \sim \frac{A_1}{A_2} \sim \frac{B_1}{B_2} \sim \frac{C_1}{C_2} \sim 100 \quad (48)$$

which are required to obtain similar value of light neutrino mass 0.1 eV in the two models. It should be remembered that μ_s and M_L correspond to lepton number breaking scale in ISS and LSS respectively (and hence should be small). Moreover, for the purpose of comparison between the two models, we have chosen same values for M_D , M , Y_M , Y_D , Λ , and m_ν in Table 5.

V. RESULTS AND DISCUSSION

The branching ratio of $\mu \rightarrow e + \gamma$ for four randomly chosen and allowed values of non-unitary parameter η , for the three allowed vacuum alignments for ISS and LSS models, is computed for seesaw scale ~ 1 TeV. The seesaw scale plays significant role in BR of muon

μ_s	1 keV
M_D	10 GeV
M	1 TeV
y_M	0.00125
y_D	0.05
y_{μ_s}	0.01
Λ	10^3 TeV
$\langle v_s \rangle$	0.05 TeV
$\langle v_{\rho'} \rangle$	0.05 TeV
$\langle v_{\rho''} \rangle$	0.05 TeV
$\langle v_\Omega \rangle$	100 TeV
$\langle v_\zeta \rangle$	75 TeV
$\langle v_\tau \rangle$	50 TeV

(a) Scales, Yukawa couplings and various flavon VEVs in a case in ISS obtained in this work, for $K_1 = 1$ eV, $m_\nu = 0.1$ eV. Typical values as obtained in our computation $A_1=2000$, $B_1=1500$, $C_1=1000$ have been used to estimate various flavon VEVs.

M_L	10 eV
M_D	10 GeV
M	1 TeV
y_M	0.00125
y_D	0.05
y_L	0.01
Λ	10^3 TeV
$\langle v_s^\dagger \rangle$	0.4 MeV
$\langle v_{\epsilon^\dagger} \rangle$	800 TeV
$\langle v_{\kappa^\dagger} \rangle$	4 MeV
$\langle v_{\zeta^\dagger} \rangle$	4 MeV
$\langle v_{\varphi^\dagger} \rangle$	4 MeV
$\langle v'_\varphi \rangle$	800 TeV

(b) Scales, Yukawa couplings and various flavon VEVs in a case in LSS obtained in this work, for $K_2 = 1$ eV, $m_\nu = 0.1$ eV. Typical values $A_2 = B_2 = C_2 = 10$ as obtained in computation have been used to estimate various flavon VEVs.

TABLE VI

decay, and hence it is possible to obtain different value of the BR for a different value of seesaw scale. For simplicity, we used $K_1 \sim K_2 \sim 1$ eV. The results are shown in Figs. (2-4) and Tables 4 and 5, which can guide that which of the case with a particular flavon VEV and mass hierarchy can be tested or eliminated by current bounds and future sensitivities of various $BR(\mu \rightarrow e + \gamma)$ experiments. In Figs. (2-4), we have shown the BR results of only those cases that give values of BR allowed by bounds of MEG, and sensitivity limits of MEG II and NG (next generation) experiments. The following observations are in order :

For same values of m_ν , seesaw scale, Dirac mass M_D , Yukawas, cut-off scale Λ (as explained in section 4.3), from the results in Tables 4-5 and Figs. (2-4), it is seen that:

1. The $\text{BR}(\mu \rightarrow e + \gamma)$ in both the seesaw models depends on the chosen value of the non-unitarity parameter η , triplet flavon VEV alignment and MH of light neutrinos.

2. For higher values of η , the BR in LSS is generally smaller/larger than that in ISS for NH/IH case, and while for smaller values of η , the BR in LSS is larger than that in ISS for both hierarchies.

3. It is observed that the BR as computed in our work, for $\eta = 5.0 \times 10^{-7}$, VEV of $\Phi_s(-1,1,1)/\text{NH}$ and $(0,1,-1)/\text{IH}$ for ISS show closest agreement with the current bounds of MEG and sensitivity limits of MEG II experiment, and this validates our model. Hence, when neutrino MH is fixed in future, one may pinpoint the favoured VEV alignment of triplet flavon ϕ_s .

4. However, the BR for lower values of $\eta = 9.0 \times 10^{-9}$ will be testable at next generation experiments only, as their BR values lie beyond the sensitivity limits of planned experiment like MEG II as well. Hence our predictions for these cases may be tested at next generation experiments.

5. When light neutrino mass and hierarchy is fixed in future by some other experiments, then through our results presented here, it would be possible to discriminate among the two models, i.e. which one out of LSS/ISS would be more favorable as preferred by results of cLFV experiments. It would also be possible to pinpoint the favorable VEV alignment of the triplet flavon.

6. Flavon VEVs, and (hence flavour symmetry breaking scale) show a rich variation of scales, as is seen from results in Table 5, and will be testable in future experiments.

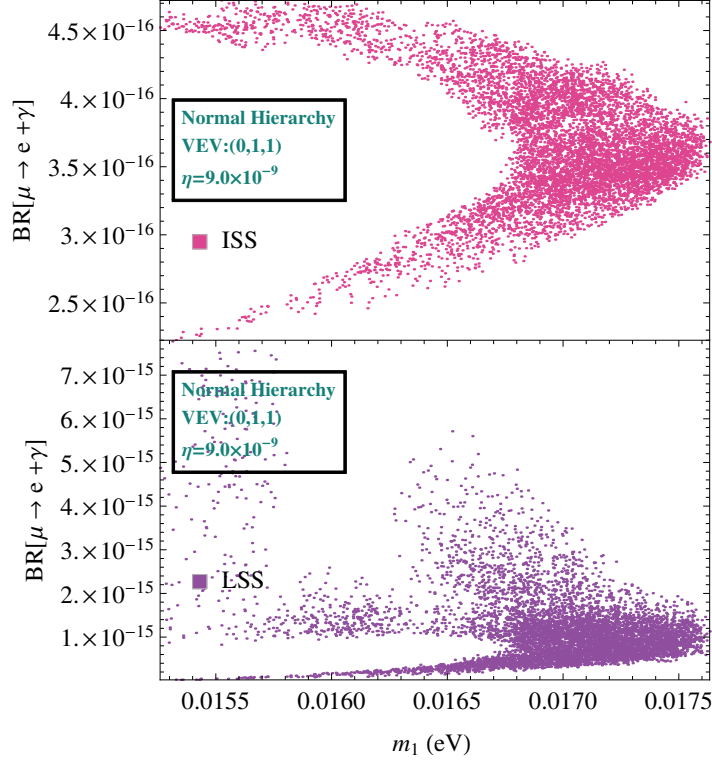


FIG. 2: Correlation plot between $BR(\mu \rightarrow e + \gamma)$ and non-unitary parameter η for allowed vacuum alignment $(0,1,1)$, Φ_s of triplet scalar field involved in both the inverse and linear seesaw models with normal hierarchy for non-unitary parameter $\eta = 9.0 \times 10^{-9}$. These BR values will be testable at NG experiments.

VI. SUMMARY AND CONCLUSIONS

In this work, we explored the feasibility of cLFV ($\mu \rightarrow e + \gamma$) decay in ISS and LSS models with A_4 symmetry, and presented detailed analysis to pinpoint that which of the models could be more favourable for testing at $(\mu \rightarrow e + \gamma)$ experiments. A few extra cyclic groups Z_4 , Z_5 and global symmetry $U(1)_x$ were used to forbid contributions from unwanted terms to neutrino mass and ensuring only the contributions that generate the desired neutrino mass matrix for the two seesaw mechanisms. In our previous work [1, 2], we found that only six VEV alignments of the triplet flavon Φ_s - $(0,1,1)/(0,-1,-1)$ and $(-1,1,1)/(1,-1,-1)$ for normal hierarchy and $(0,-1,1)/(0,1,-1)$ for inverted hierarchy are allowed such that the unknown light neutrino oscillation parameters lie within their 3σ range, for A_4 based inverse and linear seesaw models (with a tolerance of $< 10^{-5}$ for the all solutions).

In this work we used these results and computed the branching ratio of $(\mu \rightarrow e + \gamma)$. We did this for seesaw scale ~ 1 TeV, $K_1 = K_2 = 1$ eV, $Y_{\mu_s} \sim 0.01$, $M_D \sim 10$ GeV, $\mu_s \sim 1$ keV, $M \sim 1$ TeV, $m_\nu \sim 0.1$ eV, $\Lambda = 10^3$ TeV, $M_L = 1$ eV and $Y_D = 0.05$. We also chose some random values of the non-unitarity parameter η within its currently allowed range. Flavon VEVs, and (hence flavour symmetry breaking scale) show a rich variation of scales, as is seen from results in Table 5. We found that out of all cases in Table 4, for ISS, and for $\eta = 5.0 \times 10^{-7}$, VEV of $\Phi_s(-1,1,1)/\text{NH}$ and $(0,1,-1)/\text{IH}$ cases show closest agreement with the current bounds of MEG and sensitivity limits of MEG II experiment. So, the results of these cases validate our model. However, the BR for a lower value of $\eta = 9.0 \times 10^{-9}$ will be testable at next generation experiments only, as their BR values lie beyond the sensitivity limits of planned experiment like MEG II. Other cases in Table 4. are ruled out as the BR projected by them is very high, and lies beyond the current limits of MEG experiment too. It must be noted that decay rate of muon depends on the chosen value of the non-unitarity parameter η , flavon VEV alignment and MH of light neutrinos as well, hence, using the methodology of this work, and from future measurements at MEG II, it would be possible to pinpoint that which of the seesaw model, seesaw scale and VEV alignment of the triplet flavon is more favourable. Thus, the results of this work can throw light on dynamics of flavour symmetry as well as can help discriminate between LSS and ISS models, in context of cLFV decay $(\mu \rightarrow e\gamma)$. Such computation can be done for other values of flavour symmetry breaking scale, couplings too and can be constrained with the current limits and sensitivity of cLFV experiments, which can tell about which of the two models/flavon VEV will be more favourable.

Acknowledgements

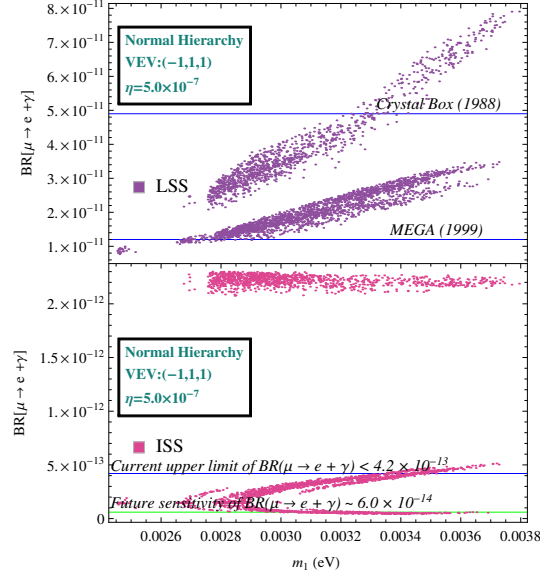
Authors acknowledge support from FIST grant SR/FST/PSI-213/2016(C) dtd. 24/10/2017(Govt. of India) in upgrading the computer laboratory of the department where part of this work was done.

[1] M. R. Devi and K. Bora, [arXiv:2103.10065 [hep-ph]], presented at DAE HEP symposium, Jatni, Odisha, December 2020.

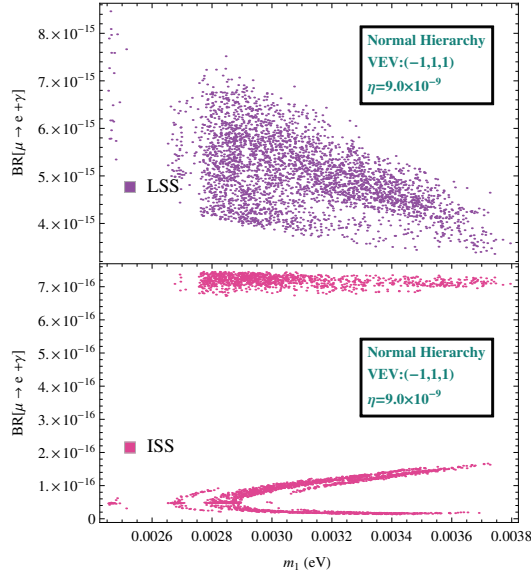
- [2] M. R. Devi and K. Bora, Mod. Phys. Lett. A, Vol **37**, No. 12, 2250073 (20 pages), doi:10.1142/S0217732322500730 [arXiv:2112.13004 [hep-ph]].
- [3] A. M. Baldini, F. Cei, C. Cerri, S. Dussoni, L. Galli, M. Grassi, D. Nicolo, F. Raffaelli, F. Sergiampietri and G. Signorelli, *et al.* [arXiv:1301.7225 [physics.ins-det]].
- [4] A. M. Baldini *et al.* [MEG], Eur. Phys. J. C **76** (2016) no.8, 434 doi:10.1140/epjc/s10052-016-4271-x [arXiv:1605.05081 [hep-ex]].
- [5] P. W. Cattaneo [MEG II], JINST **12** (2017) no.06, C06022 doi:10.1088/1748-0221/12/06/C06022 [arXiv:1705.10224 [physics.ins-det]].
- [6] P. R. Kettle, Hyperfine Interact. **214** (2013) no.1-3, 47-54 doi:10.1007/s10751-013-0789-6
- [7] M. Aoki *et al.* [C. Group], Contribution to 2022 Snowmass Summer Study, [arXiv:2203.08278 [hep-ex]].
- [8] M. Aiba, A. Amato, A. Antognini, S. Ban, N. Berger, L. Caminada, R. Chislett, P. Crivelli, A. Crivellin and G. D. Maso, *et al.* [arXiv:2111.05788 [hep-ex]].
- [9] F. Deppisch, H. Pas, A. Redelbach, R. Ruckl and Y. Shimizu, Eur. Phys. J. C **28** (2003), 365-374 doi:10.1140/epjc/s2003-01184-6 [arXiv:hep-ph/0206122 [hep-ph]].
- [10] S. Mandal, O. G. Miranda, G. Sanchez Garcia, J. W. F. Valle and X. J. Xu, Phys. Rev. D **105** (2022) no.9, 095020 doi:10.1103/PhysRevD.105.095020 [arXiv:2203.06362 [hep-ph]].
- [11] F. Deppisch, H. Päs, A. Redelbach and R. Rückl, Springer Proc. Phys. **98** (2005), 27-38 doi:10.1007/3-540-26798-0_3 [arXiv:hep-ph/0403212 [hep-ph]].
- [12] G. Hesketh *et al.* [Mu3e], Contribution to 2022 Snowmass Summer Study, [arXiv:2204.00001 [hep-ex]].
- [13] J. De Blas *et al.* [Muon Collider], Contribution to 2022 Snowmass Summer Study, [arXiv:2203.07261 [hep-ph]].
- [14] J. P. Bu, Y. M. Liang and X. W. Gu, Can. J. Phys. **92** (2014) no.12, 1587-1591 doi:10.1139/cjp-2013-0517
- [15] S. Pascoli and Y. L. Zhou, JHEP **10**, 145 (2016) doi:10.1007/JHEP10(2016)145 [arXiv:1607.05599 [hep-ph]].
- [16] L. Heinrich, H. Schulz, J. Turner and Y. L. Zhou, JHEP **04**, 144 (2019) doi:10.1007/JHEP04(2019)144 [arXiv:1810.05648 [hep-ph]].
- [17] P. F. de Salas, D. V. Forero, S. Gariazzo, P. Martínez-Miravé, O. Mena, C. A. Ternes, M. Tortola and J. W. F. Valle, JHEP **02** (2021), 071 doi:10.1007/JHEP02(2021)071 [arXiv:2006.11237

- [hep-ph]].
- [18] D. N. Dinh, N. Anh Ky, P. Q. V  n and N. T. H. V  n, [arXiv:1602.07437 [hep-ph]].
 - [19] M. C. Chen, J. Huang, J. M. O'Bryan, A. M. Wijangco and F. Yu, JHEP **02** (2013), 021 doi:10.1007/JHEP02(2013)021 [arXiv:1210.6982 [hep-ph]].
 - [20] R. Kalita, D. Borah, Phys. Rev. D **92** (2015) no.5, 055012 doi:10.1103/PhysRevD.92.055012 [arXiv:1508.05466 [hep-ph]].
 - [21] N. Sarma, K. Bora and D. Borah, Eur. Phys. J. C **79** (2019) no.2, 129 doi:10.1140/epjc/s10052-019-6584-z [arXiv:1810.05826 [hep-ph]].
 - [22] M. Hirsch, S. Morisi and J. W. F. Valle, Phys. Lett. B **679** (2009), 454-459 doi:10.1016/j.physletb.2009.08.003 [arXiv:0905.3056 [hep-ph]].
 - [23] M. Sruthilaya, R. Mohanta and S. Patra, Eur. Phys. J. C **78** (2018) no.9, 719 doi:10.1140/epjc/s10052-018-6181-6 [arXiv:1709.01737 [hep-ph]].
 - [24] D. Borah and B. Karmakar, Phys. Lett. B **780** (2018), 461-470 doi:10.1016/j.physletb.2018.03.047 [arXiv:1712.06407 [hep-ph]].
 - [25] P. Sahu, S. Patra and P. Pritimita, [arXiv:2002.06846 [hep-ph]].
 - [26] G. Altarelli and F. Feruglio, Nucl. Phys. B **741** (2006), 215-235 doi:10.1016/j.nuclphysb.2006.02.015 [arXiv:hep-ph/0512103 [hep-ph]].
 - [27] L. Calibbi and G. Signorelli, Riv. Nuovo Cim. **41** (2018) no.2, 71-174 doi:10.1393/ncr/i2018-10144-0 [arXiv:1709.00294 [hep-ph]].
 - [28] S. M. Bilenky, S. T. Petcov and B. Pontecorvo, Phys. Lett. B **67** (1977), 309 doi:10.1016/0370-2693(77)90379-3
 - [29] R. Lal Awasthi and M. K. Parida, Phys. Rev. D **86** (2012), 093004 doi:10.1103/PhysRevD.86.093004 [arXiv:1112.1826 [hep-ph]].
 - [30] M. K. Parida and B. P. Nayak, Adv. High Energy Phys. **2017** (2017), 4023493 doi:10.1155/2017/4023493 [arXiv:1607.07236 [hep-ph]].
 - [31] B. He, T. P. Cheng and L. F. Li, Phys. Lett. B **553** (2003), 277-283 doi:10.1016/S0370-2693(02)03258-6 [arXiv:hep-ph/0209175 [hep-ph]].
 - [32] L. Delle Rose, C. Marzo and A. Urbano, JHEP **12** (2015), 050 doi:10.1007/JHEP12(2015)050 [arXiv:1506.03360 [hep-ph]].
 - [33] D. V. Forero, S. Morisi, M. Tortola and J. W. F. Valle, JHEP **09** (2011), 142 doi:10.1007/JHEP09(2011)142 [arXiv:1107.6009 [hep-ph]].

- [34] X. Marcano Imaz, Springer theses, doi:10.1007/978-3-319-94604-7 [arXiv:1710.08032 [hep-ph]].
- [35] M. J. Dolan, T. P. Dutka and R. R. Volkas, JCAP **06** (2018), 012 doi:10.1088/1475-7516/2018/06/012 [arXiv:1802.08373 [hep-ph]].
- [36] T. P. Cheng and L. F. Li, *Gauge theory of elementary particle physics: Problems and solutions*. 2000. Oxford, UK: Clarendon (2000) 306 p.
- [37] A. Ilakovac and A. Pilaftsis, Nucl. Phys. B **437** (1995), 491 doi:10.1016/0550-3213(94)00567-X [arXiv:hep-ph/9403398 [hep-ph]].
- [38] R. Alonso, M. Dhen, M. B. Gavela and T. Hambye, JHEP **01** (2013), 118 doi:10.1007/JHEP01(2013)118 [arXiv:1209.2679 [hep-ph]].
- [39] H. c. Han and Z. z. Xing, Nucl. Phys. B **973** (2021), 115609 doi:10.1016/j.nuclphysb.2021.115609 [arXiv:2110.12705 [hep-ph]].
- [40] B. Karmakar and A. Sil, Phys. Rev. D **96**, no.1, 015007 (2017) doi:10.1103/PhysRevD.96.015007 [arXiv:1610.01909 [hep-ph]].
- [41] P. S. B. Dev and R. N. Mohapatra, Phys. Rev. D **81** (2010), 013001 doi:10.1103/PhysRevD.81.013001 [arXiv:0910.3924 [hep-ph]].
- [42] E. K. Akhmedov, M. Lindner, E. Schnapka and J. W. F. Valle, Phys. Lett. B **368** (1996), 270-280 doi:10.1016/0370-2693(95)01504-3 [arXiv:hep-ph/9507275 [hep-ph]].
- [43] M. Malinsky, J. C. Romao and J. W. F. Valle, Phys. Rev. Lett. **95** (2005), 161801 doi:10.1103/PhysRevLett.95.161801 [arXiv:hep-ph/0506296 [hep-ph]].
- [44] F. F. Deppisch, L. Graf, S. Kulkarni, S. Patra, W. Rodejohann, N. Sahu and U. Sarkar, Phys. Rev. D **93** (2016) no.1, 013011 doi:10.1103/PhysRevD.93.013011 [arXiv:1508.05940 [hep-ph]].
- [45] E. Fernandez-Martinez, J. Hernandez-Garcia and J. Lopez-Pavon, JHEP **08** (2016), 033 doi:10.1007/JHEP08(2016)033 [arXiv:1605.08774 [hep-ph]].
- [46] Y. Wang and S. Zhou, Phys. Lett. B **824** (2022), 136797 doi:10.1016/j.physletb.2021.136797 [arXiv:2109.13622 [hep-ph]].
- [47] I. Baldes, N. F. Bell, K. Petraki and R. R. Volkas, JCAP **07** (2013), 029 doi:10.1088/1475-7516/2013/07/029 [arXiv:1304.6162 [hep-ph]].

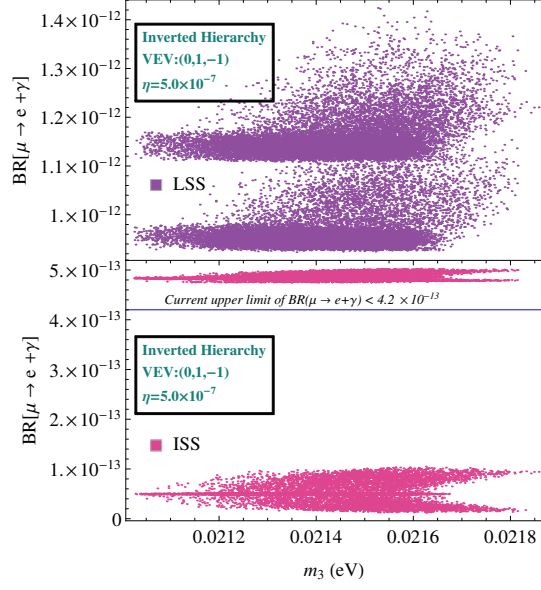


(a)

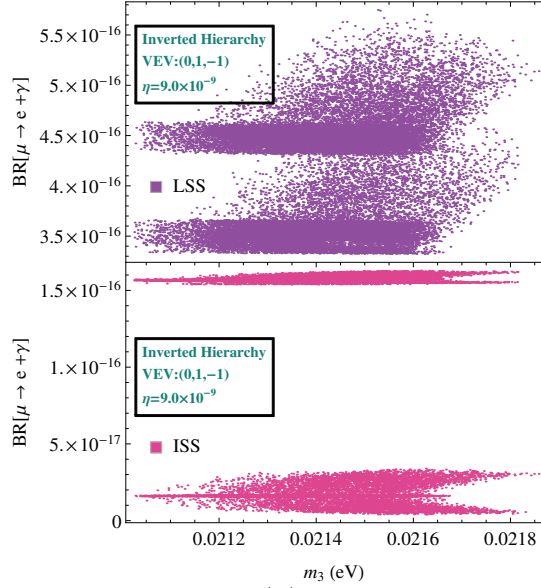


(b)

FIG. 3: Correlation plot between $BR(\mu \rightarrow e + \gamma)$ and non-unitary parameter η for allowed vacuum alignment $(-1,1,1)$ of triplet scalar field, Φ_s involved in (a) inverse seesaw model for normal hierarchy with non-unitary parameter, $\eta = 5.0 \times 10^{-7}$, these BR values will be testable at MEG and MEG II experiments and (b) for both the inverse and linear seesaw models with normal hierarchy for $\eta = 9.0 \times 10^{-9}$, these BR values will be testable at NG experiments.

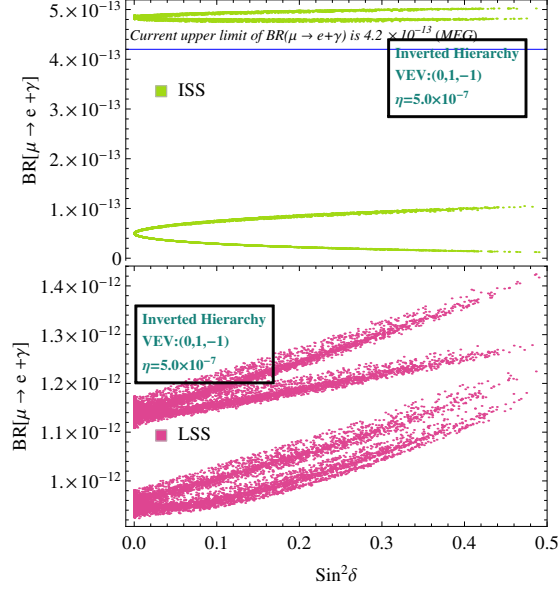


(a)

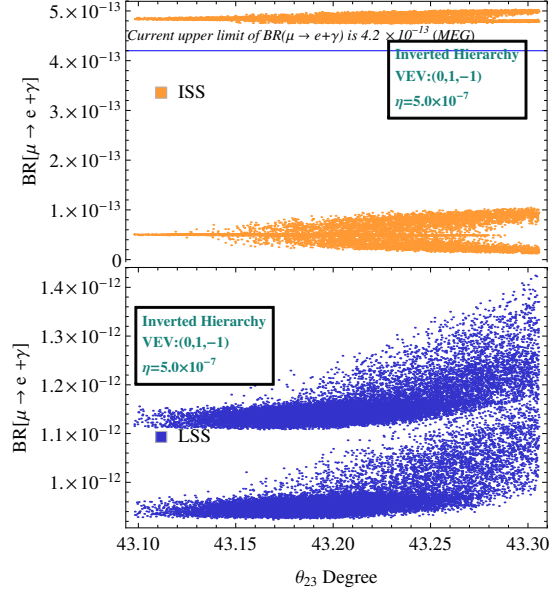


(b)

FIG. 4: Correlation plot between $BR(\mu \rightarrow e + \gamma)$ and non-unitary parameter η for allowed vacuum alignment $(0,1,-1)$ of triplet scalar field, Φ_s involved in (a) inverse seesaw model for inverted hierarchy with non-unitary parameter, $\eta = 5.0 \times 10^{-7}$, these BR values lie within allowed limits of MEG experiment and (b) for both the inverse and linear seesaw models with inverted hierarchy for $\eta = 9.0 \times 10^{-9}$, these BR values will be testable at NG experiments.

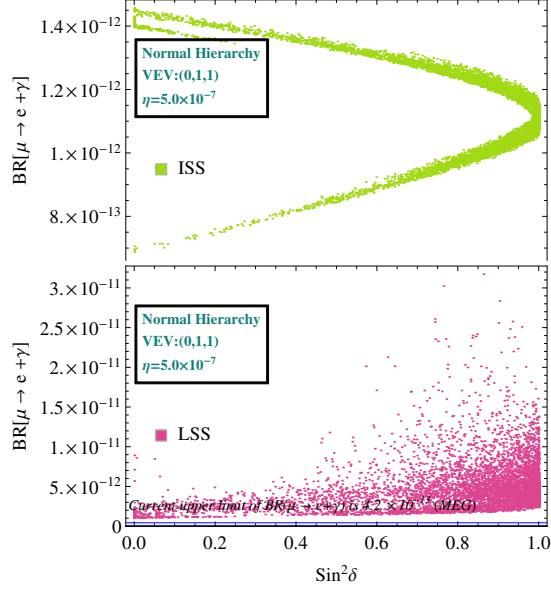


(a)

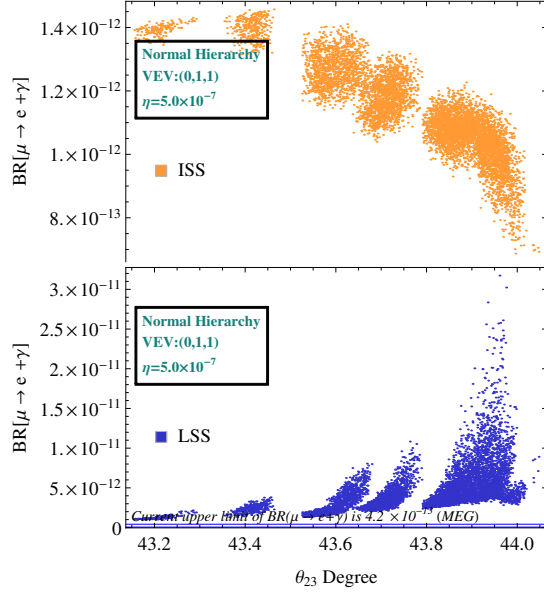


(b)

FIG. 5: (a) Correlation plot between $BR(\mu \rightarrow e + \gamma)$ and $\text{Sin}^2\delta$ and (b) Correlation plot between $BR(\mu \rightarrow e + \gamma)$ and θ_{23} for allowed vacuum alignment (0,1,-1) of triplet scalar field, Φ_s involved in both the inverse and linear seesaw models with inverted hierarchy with non-unitary parameter, $\eta = 5.0 \times 10^{-7}$.

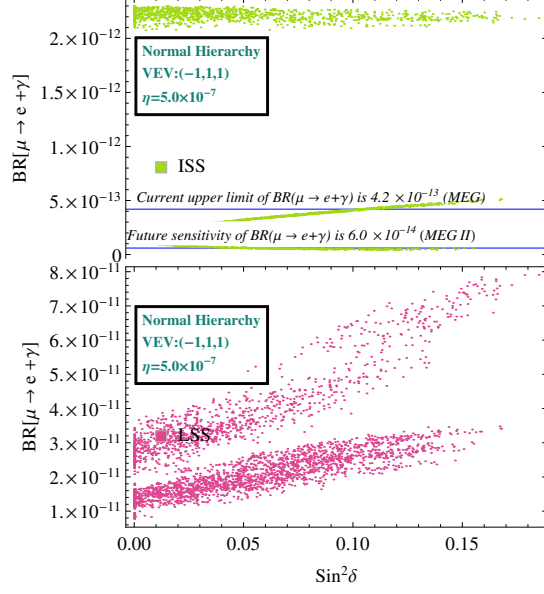


(a)

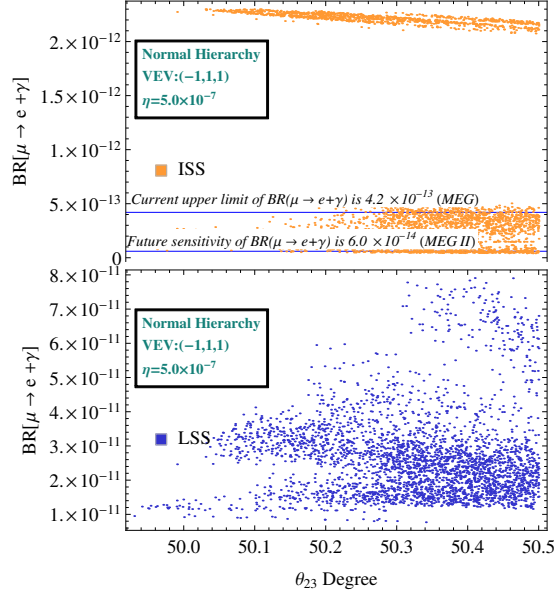


(b)

FIG. 6: (a) Correlation plot between $BR(\mu \rightarrow e + \gamma)$ and $\text{Sin}^2\delta$ and (b) Correlation plot between $BR(\mu \rightarrow e + \gamma)$ and θ_{23} for allowed vacuum alignment (0,1,1) of triplet scalar field, Φ_s involved in both the inverse and linear seesaw models with normal hierarchy with non-unitary parameter, $\eta = 5.0 \times 10^{-7}$.



(a)



(b)

FIG. 7: (a) Correlation plot between $BR(\mu \rightarrow e + \gamma)$ and $\text{Sin}^2\delta$ and (b) Correlation plot between $BR(\mu \rightarrow e + \gamma)$ and θ_{23} for allowed vacuum alignment $(-1, 1, 1)$ of triplet scalar field, Φ_s involved in both the inverse and linear seesaw models with normal hierarchy with non-unitary parameter, $\eta = 5.0 \times 10^{-7}$.